J4.5 APPLICATIONS AND ACCURACY OF RADIO OCCULTATION OBSERVATIONS USING GPS

E. Robert Kursinski[1], George Hajj and Stephen S. Leroy
Jet Propulsion Laboratory, California Institute of Technology
Pasadena, CA 91109

1. INTRODUCTION

The radio occultation technique has been used to characterize planetary atmospheres since the 1960's spanning atmospheric pressures from several bars to 16 microbars. While observing Earth's atmosphere via radio occultation was conceived in 1960's, the major breakthrough in realization came with the idea of using GPS signals for occultation observations [Yunck et al., 1988] by solving the prohibitive space-borne transmitter cost. GPS provides the ability to limb sound the atmosphere from the mesosphere to the surface. We summarize and highlight some of the results to date in this evolving area.

2. BACKGROUND

The GPS to low-Earth-orbiter occultation geometry is shown in Figure 1. Relative motion between the transmitter and receiver produce a limb scan of the atmosphere in roughly 60 seconds.

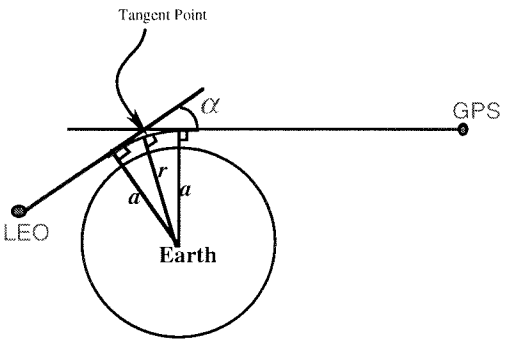

Figure 1. GPS occultation geometry

From measurements of Doppler shift and knowledge of changing viewing geometry, the bending angle, α, as a function of asymptotic miss distance, a, is derived. The index of refraction, n, as a function of radius from the center of curvature, r, is derived from $\alpha(a)$ via an Abelian integral transform relation under the assumption of local spherical symmetry [Fjeldbo et al., 1971]. Therefore each occultation yields a profile of refractivity (defined as $N = [n\text{-}1]\ 10^6$) versus height. At microwave wavelengths refractivity is given as

$$N = b_1 \frac{P}{T} + b_2 \frac{P_w}{T^2} \qquad (1)$$

where P is pressure, P_w is partial pressure of water vapor, T is temperature and b_1 and b_2 are constants equal to 77.6 K mb^{-1} and 3.73x10^5 K^2 mb^{-1} respectively. Because of its permanent dipole moment, each water vapor molecule contributes approximately 15 to 20 times the refractivity of an average dry (N_2 or O_2) molecule and water therefore contributes significantly to refractivity in the lower troposphere. In the cold, dry conditions of the upper troposphere and above (T<250K) water contributes little to refractivity and profiles of refractivity are directly proportional to density. Hydrostatically integrating density yields a profile of pressure (or equivalently geopotential), and knowing density and pressure yields temperature. Given additional temperature information, water vapor can be derived in the middle and lower troposphere.

3. COVERAGE AND RESOLUTION

A single orbiting GPS receiver can observe between 500 and 700 daily occultations distributed globally (Figure 2), a number which can be doubled by adding the ability to receive signals from the Russian GLONASS satellites. Therefore a single receiver can provide daily as many high vertical resolution soundings as the present global radiosonde network, but with a far more even distribution of coverage.

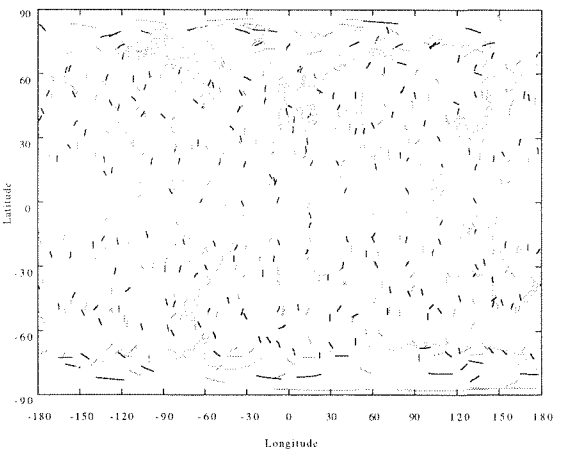

Figure 2. Distribution of occultations observed in one day by a receiver in low Earth orbit viewing 24 GPS satellites

The limb-viewing geometry of the occultation observations creates a pencil-like sampling volume with vertical and cross-track resolution of order 1 km and along-track resolution of order 100-300 km. Vertical and cross-track resolution is defined by Fresnel diffraction. Figure 3 shows an example of vertical resolution defined as the diameter of the first Fresnel zone estimated from a radiosonde profile from Hilo, Hawaii on July 11, 1991, at 12:00 UT [Kursinski et al., 1997]. In the mid-

[1] E. Robert Kursinski, MS 238-600, Jet Propulsion Laboratory, Pasadena, CA, 91109
e-mail: erk@mercu1.caltech.edu

stratosphere and above, vertical resolution is 1.4 km. Deeper in the atmosphere, increased bending causes the vertical dimension of the first Fresnel zone to shrink. Sharp structures below 10 km altitude are associated with water vapor layers. The impact of the enormous vertical refractivity gradient at the tradewind inversion near 4 km is evident. Resolution improves to ~150 m on the top side of the inversion and decreases on the bottom side associated with focusing there.

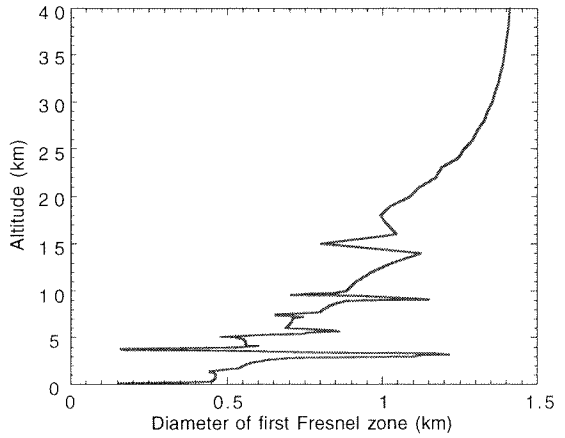

Figure 3. Vertical resolution of GPS occultations [Kursinski et al., 1997]

4. PREDICTED ACCURACY

We have identified and quantified a number of important sources of error in the occultation measurement and retrieval process which are summarized below.

4.1 *Temperature Errors*

Figure 4 shows the estimated root-mean-square (rms) temperature errors for individual profiles [Kursinski et al., 1997]. Differences at middle atmospheric altitudes between Figures 4a and 4b are due primarily to higher signal to noise ratio at the GPS receiver and night time ionosphere conditions assumed in Figure 4a. Less accurate results in the lower troposphere in Figure 4b reflect the influence of water vapor at low latitudes whereas Figure 4a reflects high latitude conditions. Figures 4a and 4b assume tropospheric water vapor is known to 20%. In the upper troposphere-lower stratosphere, the dominant error is the spherical symmetry assumption. Note that estimated errors in retrieved temperature are sub-Kelvin from the upper troposphere into the lower stratosphere.

4.2 *Geopotential Errors*

Figure 5 shows the estimated error in geopotential heights of pressure surfaces derived from the GPS observations. The primary difference between Figures 5a and 5b in the middle atmosphere is the nightime versus daytime ionosphere. In the troposphere the difference represents the impact of

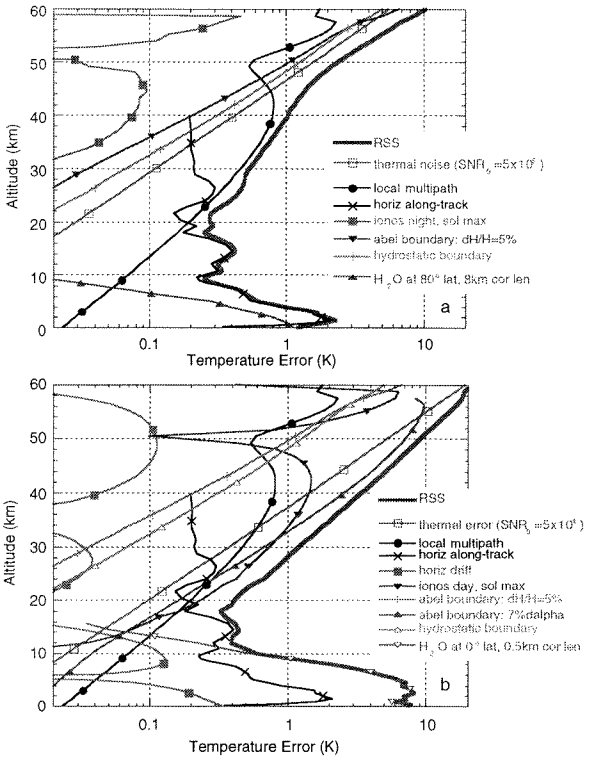

Figure 4. Predicted errors in temperatures derived from GPS occultation profiles. a - Night time, high SNR and high latitude, b - Daytime, low SNR and low latitude [Kursinski et al., 1997]

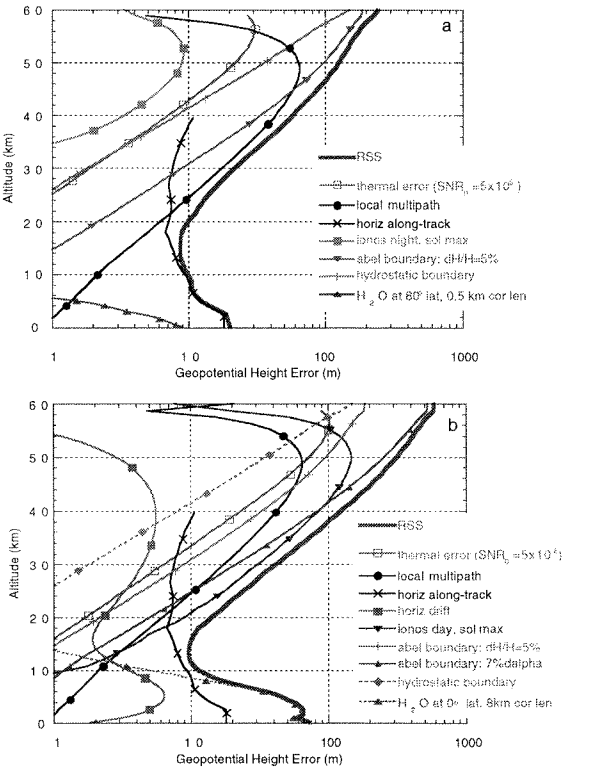

Figure 5. Estimated error in geopotential height of pressure surfaces for the same conditions of Figure 4. [Kursinski et al., 1997]

water vapor at high versus low latitudes analogous to Figures 4a and 4b. Errors are estimated to be 10 to 20 m rms in the lower stratosphere through upper troposphere where the error associated with the spherical symmetry assumption dominates. Small errors extend to the surface at high latitudes where the air is cold and dry.

4.3 *Water Vapor Errors*

The accuracy of water vapor derived from GPS refractivity profiles depends primarily on the accuracy of assumed temperature and retrieved refractivity. Figure 6 reflects expected rms error of individual water vapor profiles for annual mean conditions based on the climatology of Peixoto and Oort [1992] assuming temperature is known to 1.5 K rms. Accuracy is primarily limited by the temperature accuracy above 4 km (~600 mb). At lower altitudes, refractivity errors increase because horizontal water vapor variations reduce the accuracy of the spherical symmetry approximation. At low latitudes, profiles of water vapor derived from occultation observations should be accurate to ~5% or better within the convective boundary layer and better than 20% below 6 to 7 km. The bias in the water vapor profiles of relevance to climate-related research will depend primarily on the accuracy of assumed temperature.

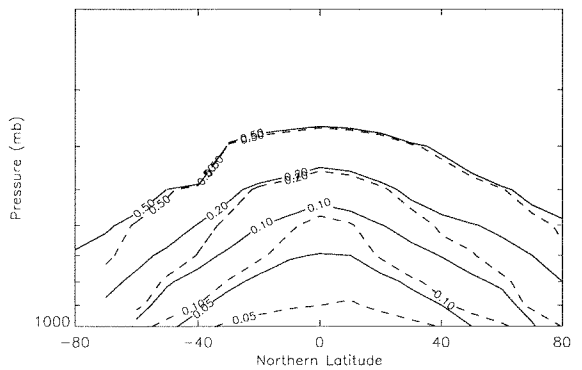

Figure 6. Estimated rms fractional error of individual derived water vapor profiles for annual mean conditions. Solid lines contain the temperature and pressure uncertainty contributions only. Dashed lines include the lower troposphere refractivity error as well. [Kursinski et al., 1995]

5. INITIAL RESULTS

Acquisition of the first GPS occultation data set commenced with the launch of the prototype GPS occultation mission, GPS/MET, in April, 1995 [Ware et al., 1996]. We have derived temperature, geopotential and water vapor results from GPS/MET data. Retrievals were initialized at 50 km extrapolating an exponential model of bending angle to higher altitudes for the abelian integral and assuming a climatological temperature at 50 km to initialize the hydrostatic integral. Due to the sparsity of the occultation profiles and radiosonde locations, results have been compared with the nearest 6 hour global analyses from the European Center for Medium-Range Weather Forecasts (ECMWF) interpolated to the occultation locations.

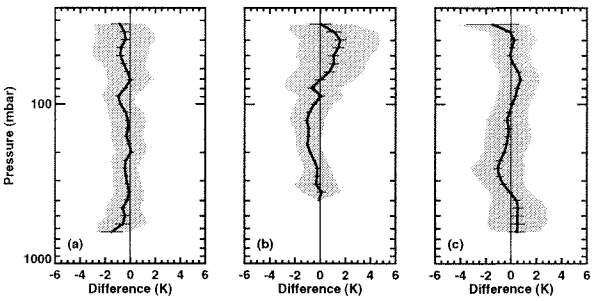

Figure 7. Comparisons between the ECMWF analyses and temperature profiles retrieved from radio occultations on 4th and 5th May, 1995. The panels plot mean temperature differences (retrieved-ECMWF) for (a) 34 profiles in the northern hemisphere (> 30°N), (b) 32 profiles in the tropics (30°S to 30°N), and (c) 33 profiles in the southern hemisphere (> 30°S). The vertical curve represents mean temperature differences and the horizontal error bars depict the standard error in the mean. The shaded area is defined by the mean temperature difference plus or minus the standard deviation of the temperature difference about the mean. [Kursinski et al. 1996]

5.1 *Temperature*

Figure 7 shows a statistical comparison between the ECMWF and GPS-derived temperatures. The lowest altitude of the data comparison is defined at the point where the temperature reaches 250K in the troposphere which avoids the water vapor ambiguity in interpretting the source of the retrieved refractivity. In the northern hemisphere where the analyses are presumed most accurate, mean differences are generally with 0.5K and standard deviations are within 1K. The cause of the vertical structure in the tropical upper troposphere is unclear. The large scatter in the tropical lower stratosphere is due to waves which are resolved in the GPS data but not in the analyses. The southern hemisphere profiles were found to separate into two rather distinct groups shown in Figure 8. While most of the GPS and ECMWF profiles were in close agreement,

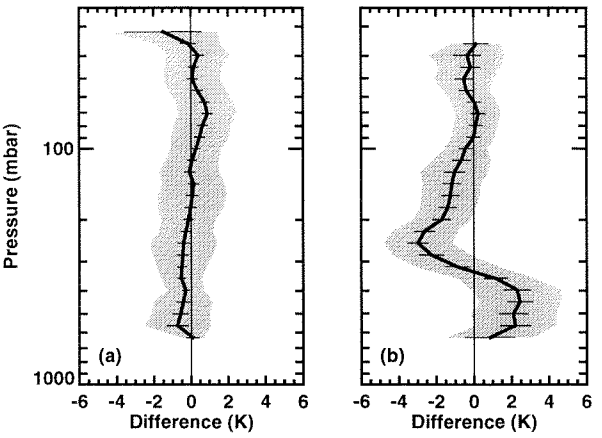

Figure 8. Statistical comparison of the 33 southern hemisphere profiles from April-May 1995 period divided into two groups: (a) 25 profiles which differ little relative to the model and (b) 8 profiles with the largest deviations relative to the model. [Kursinski et al., 1996]

about one quarter of the profiles indicated the troposphere was too cold and the tropopause was too low in altitude in the analyses. All but one of the erroneous profiles was located in the southeastern Pacific, a region devoid of land mass and radiosondes.

5.2 *Geopotential*

Figure 9 shows a statistical comparison between ECMWF and GPS-derived geopotential for June 21 to July 4, 1995, analogous to Figure 7. Biases in the mean are 10 to 20 m in the northern hemisphere and almost zero in the tropics. Standard deviations in the northern hemisphere and tropics are ~20 m, roughly a

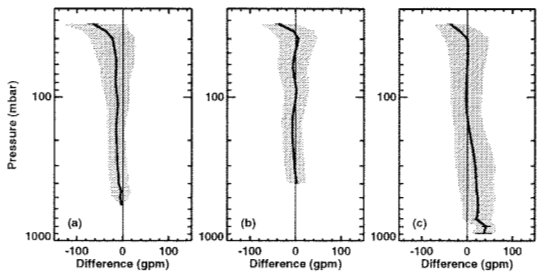

Figure 9 Statistical comparison of geopotential height derived from GPS/MET data taken during the June-July period of 1995. [Leroy, 1997]

factor of 2 larger than the predicted rms errors in Figure 5 indicating the prototype GPS/MET system is performing quite well in this regard. Reduced agreement in the southern hemisphere is consistent with sparse radiosonde data. The structure of the mean difference with agreement in the lower stratosphere and ~constant positive bias in the troposphere imply ECMWF temperatures are too cold near the tropopause and surface pressure is too high.

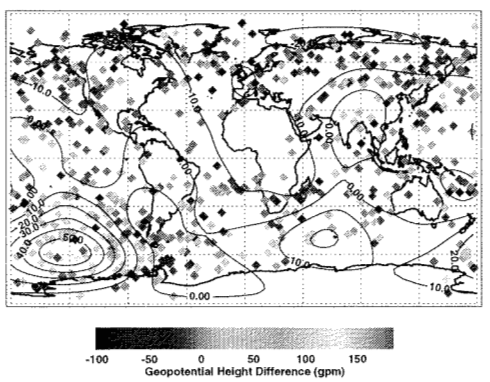

Figure 10 Geopotential height difference at 300 mb: Occultation - ECMWF June 21 - July 4, 1995. Contours are at 10 gpm intervals [Leroy, 1997]

Figure 10 shows a low order spherical harmonic fit to the difference between ECMWF and GPS-derived geopotential height of the 300 mb pressure surface. Systematic differences in behavior, are particularly apparent in the southeastern Pacific where the analyses exhibit a systematically cold bias in the troposphere.

5.3 *Water Vapor*

We have derived some initial water vapor profiles from GPS/MET data using the interpolated ECMWF temperature field to isolate the water vapor contribution to refractivity in equation (1). Derivation of water vapor begins when the GPS profile temperature reaches 230 K in the troposphere. Figure 11 shows the zonal mean specific humidity derived from the June 21 to July 4, 1995, span of GPS/MET data consisting of 660 occultations. Major features include the large summer-winter hemisphere contrast, peak humidities near the inter-tropical convergence zone (ITCZ) between 5°N and 10°N, the dry descending branch of the Hadley circulation between 10°S and 20°S and high mean specific humidities near 30°N above 7 km associated with the southeast Asian monsoon. Also of note is the fact that many profiles extend to within 1 km of the surface indicating the ability of GPS to probe the lower troposphere.

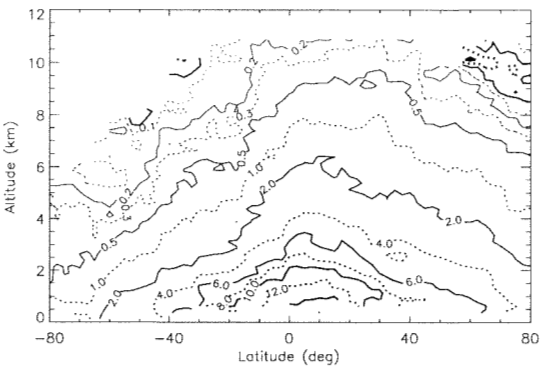

Figure 11 Zonal mean specific humidity in g/kg for June 21 to July 4, 1995 derived from GPS occultation data and ECMWF temperature data.

Figure 12 shows the mean of the differences between the occultation-derived and ECMWF specific humidity fields. Agreement is ~0.1 g/kg in the upper regions. The GPS results suggest the atmosphere below the 500 mb level is somewhat drier in general than the ECMWF humidity field except in the vicinity of the ITCZ near 2 km altitude. ECMWF analyses are far more moist near the tradewind inversion between 0 and 30S. Examination of individual profiles reveals that the ECMWF analyses are smoothing out the vertical structure of the tradewind inversion and extending boundary layer air too high in altitude. The biases between ECMWF and occultation humidity fields may also indicate the tropical Hadley circulation is too weak in the analyses

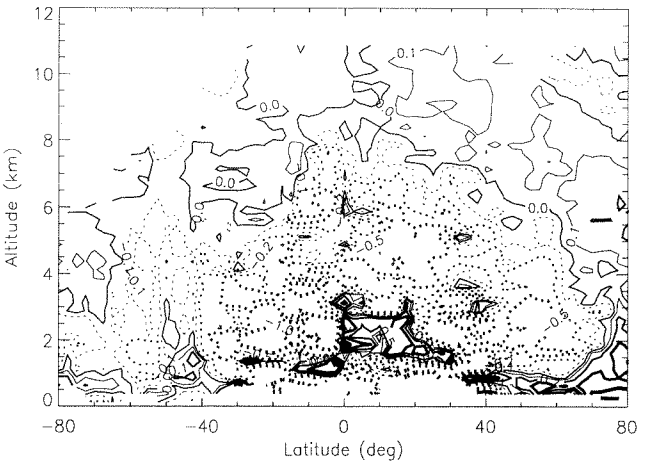

Figure 12 Zonal mean difference between GPS occultation derived specific humidity and specific humidity from the ECMWF analyses. Dotted lines are negative. Solid lines are nonnegative

6. APPLICATIONS

GPS occultations provide a unique combination of vertical resolution, global distribution, insensitivity to clouds and precipitation and high accuracy of individual profiles for weather as well as long term stability for climate. Given their importance to cyclogenesis, upper troposphere temperature and geopotential structure derived from GPS should prove useful particularly in regions inaccessible by radiosondes such as oceanic regions like the north Atlantic storm track and most of the southern hemisphere. Low level moisture is important in storm genesis and evolution as well particularly at lower latitudes in oceanic regions. Kuo et al. [1996] demonstrated the impact of assimilating GPS observations into a model for capturing the evolution of an extratropical cyclone. Both the upper level constraints on temperature and geopotential and the low level constraints on moisture were important for capturing the extreme low pressure. The GPS observations offer a quantum improvement in vertical resolution on the global scale sorely needed for understanding the distribution, variability and control of moisture. While independent temperature knowledge is needed to separate the wet and dry refractivity contributions in equation (1), temperature is far better known and less variable in a fractional sense than water vapor. Further, the insensitivity to particulates yields profiles in both clear and cloudy conditions unlike IR observations.

In the context of climate, biases rather than random errors in individual profiles are important. With the exception of the ionosphere error, the errors characterized in Figures 4 and 5 should average down and biases will be perhaps an order of magnitude smaller than the errors in Figures 4 and 5. The bias in the ionosphere error should be reducable with a 2nd order ionosphere correction. To put the predicted accuracies in perspective, knowledge of the geopotential height of pressure near the tropopause to an accuracy of 1 m equates to a knowledge of average tropospheric temperature to ~0.02 K [Kursinski et al., 1997]. Work has begun on utilizing occultation data for detecting anthropogenic changes in climate.

Initial results are very promising indicative of the simplicity and robustness of the technique. Improvements continue to evolve. Changes in the occultation receiver are being developed to improve signal tracking in the lowest regions of the troposphere. Several groups are working to surpass the Fresnel diffraction resolution limit which amounts essentially to 1-D holography. Kuo and Zou at NCAR and Eyre at the Met. Office as well as otheres are developing methods to assimilate GPS occultation data into numerical weather prediction (NWP) models in 3D and 4D variational schemes including generalization to a nonspherical retrieval to take advantage of the 3D structure of the model and improve accuracy particularly in the lower troposphere [Eyre, 1994].

In the near future, four second-generation occultation receivers developed at JPL will launch into low Earth orbit such that there should be ~1500 globally distributed daily occultations available by the end of 1999. Initial results derived from GPS/MET have been sufficiently promising for a GPS occultation receiver to have been chosen as a sensor on the National Polar-orbiting Operational Environmental Satellite System (NPOESS). Eventually a large constellation of receivers may be placed in orbit on compact disk-sized spacecraft yielding tens of thousands of daily profiles to improve weather prediction.

Acknowledgements: The work presented here is the result of research supported by NASA's Mission to Planet Earth Office, internal research funds at the California Institute of Technology and recently by the Integrated Progam Office of the NPOESS.

References:

Eyre, J. R., Assimilation of radio occultation measurements into a numerical weather prediction system, *European Centre for Medium-Range Weather Forecasts,* Technical Memorandum No. 199, May, 1994.

G. Fjeldbo, A.J.Kliore and V.R.Eshleman, The neutral atmosphere of Venus as studied with Mariner V radio occultation experiments, *Astronom. J.*, 76, 123, 1971.

Kuo, Y.-H., X. Zou and W. Huang, The impact of GPS data on the prediction of an extratropical cyclone: an observing system simulation experiment, submitted to *J. Dyn. Atmos. Ocean*, February, 1996.

E.R.Kursinski, G.A.Hajj, K.R.Hardy, L.J.Romans, J.T.Schofield, Observing tropospheric water vapor by

radio occultation using the Global Positioning System, *Geophys. Res. Lett.*, 22, 2365, 1995.

E.R.Kursinski, G.A.Hajj et al., Initial results of Radio occultation observations of Earth's atmosphere using the Global Positioning System, *Science*, 271, 1107-1110, 1996.

Kursinski, E.R., G.A.Hajj, K.R.Hardy, J.T.Schofield and R.Linfield, Observing Earth's atmosphere with radio occultation measurements using GPS, to appear in *J. Geophys. Res.*, 1997.

Leroy, S.S., The measurement of geopotential heights by GPS radio occultation, *J. Geophys. Res.*, 1997.

Ware, R., et al., GPS sounding of the atmosphere from low Earth orbit - preliminary results, *Bull. Am. Met. Soc.*, 77, 19, 1996.

Yunck, T. P., G. F. Lindal and C. H. Liu, The role of GPS in precise Earth observation, *Proceedings of IEEE Position, Location and Navigation Symposium*, Orlando, FL, Nov. 29 - Dec. 2, 1988.